

XI

LIGHT SCATTERING

Optical Properties of Dust from Laboratory Scattering Measurements

Bo Å. S. Gustafson

*Department of Astronomy, 211 SSRB, University of Florida,
Gainesville, Fl 32611, U.S.A.*

Abstract. This is a description of the beginning of a systematic investigation into the optical properties of dust structures that are likely to be representative of interplanetary dust. I delineate the development of a physical dust model to parameterize the optically important characteristics of the dust. The result is a system with two refractive indexes in an aggregate structure of varying porosity - a challenging model for most current light scattering theories. Experimental data is needed to investigate the scattering by these structures and to test new theoretical solutions (e.g., Xu 1995) as they develop. I give a brief description of the new microwave analog scattering laboratory that has been developed for this purpose at the Laboratory for Astrophysics of the University of Florida's Astronomy Department. Finally, laboratory data is shown in support of dense aggregate models for interplanetary dust.

1. Introduction

Measurements of the brightness and degree of linear polarization of the Zodiacal light are usually obtained as a function of the elongation angle of the direction of sight from the sun. These observations need to be translated to a variation with the sun-observer angle at the particle (i.e., scattering angle) so that the effect of changing scattering geometry along the line of sight is removed before they can be compared to laboratory data. We need to bear in mind that this inversion process usually does not lead to a unique solution and is not likely to produce data that represent the scattering from a single type of particle (e.g., Levasseur-Regourd, these proceedings). The broad characteristics of the inverted scattering function is that of a brightness increase toward small scattering angles that is expected for particles that are larger than the wavelength. A color that is approximately neutral also supports this interpretation. However, the variation of the linear degree of polarization with scattering angle is reminiscent of that expected for smaller particles, although the polarization of $\sim 40\%$ around 90 degrees is considerably lower than for Rayleigh particles (having 100% polarization at 90 degrees). At first view, interplanetary dust therefore have some characteristics of small particles and some characteristics of large particles in the way they scatter light. Greenberg & Gustafson (1981) pointed out that their "Bird's-Nest" low porosity aggregated interstellar dust model for cometary dust produces Rayleigh-like polarization due to the size of the individual grains in the aggregate while the angular distribution of the brightness is produced mostly by

interference between the scattering contributed from individual grains and mimics a bigger particle. For this reason and because comets are believed by many to be a major contributor to the interplanetary dust complex, the "Bird's-Nest" model was also proposed as a model for interplanetary particles. Because, the interplanetary dust grains are generally larger than the approximately micron sizes that could be modeled in the available laboratory facilities, the optical properties of a large "Bird's-Nest" aggregate model representing zodiacal dust could not be tested. This was troublesome because one may suspect that color would also be more reminiscent of small particles and thus inconsistent with zodiacal dust.

With the advent of the microwave facility at the Laboratory for Astrophysics, it is now possible to investigate the scattering by dust models corresponding to 30 micron across in the visual. In addition, data is routinely obtained at 85 to 501 discrete wavelengths from 2.7 mm to 4 mm so that color data can easily be obtained over an interval as broad as the visual range. Our biggest challenge is the building of fluffy 20 cm size models consisting of 10^6 to 10^7 individual pieces of 0.5 millimeter size. Smaller models are easier to handle and we are also testing an exact theoretical solution on some of the smaller and simpler aggregates (Xu & Gustafson, this volume). The data presented in this article is for a compact aggregate in the 8 micron size range. This is our "working model" for a zodiacal dust particle representing a piece from a comet mantle rather than the fresh unprocessed material that the "Bird's-Nest" model represents. Intermediate porosity models would represent dust from D-, C-, and possibly S-type asteroids.

2. Physical Models of Interplanetary Dust

A consistent framework to model interplanetary matter and to interpret observations emerges based on a simple chronology carried back to the formation of interstellar grains following Greenberg & Gustafson (1981).

Protosolar nebula dust is thought to consist primarily of variously processed ice mantles condensed on silicate cores (e.g., Greenberg 1988). Silicate spheres are thought to grow by condensation in the outflow from cool super giant stars and may be reprocessed in the interstellar medium (Seab 1987). Aggregates develop from dust-dust collisions. The existence of interstellar polarization indicates that the classical grains responsible for most of the extinction at optical wavelengths are elongated and aligned. Aspect ratios of 1:2 to 1:3, i.e., 2 to 3 sphere arrays can reproduce the degree of polarization while the wavelength dependence of extinction (interstellar reddening) is indicative of 0.1 micron sizes (Greenberg & Hage 1990). Condensing molecules consolidate the structure by encapsulating the array in an ice mantle. Billions of years of ultraviolet photo-processing in interstellar space and cosmic-ray bombardment changes the organic laden ice into an absorbing refractory carbon-rich, oxygen-poor material.

As the solar nebula forms, excess gas is thought to condense on essentially pristine protosolar dust in the outer parts of the nebula. Water ice with inclusions of 0.01 micron grains of polycyclic aromatic hydrocarbon (PAH) dominates in this outer mantle condensed in the solar nebula. Greenberg & Hage (1990) adopted mass fractions in the outer parts of the nebula where comets form of

0.20, 0.19, 0.55, and 0.06 for the silicate, organic-refractory, volatile ice, and PAH, respectively, based on observed quantities and cosmic abundances. The corresponding densities are 3.5, 1.8, 1.2, and 2 g cm⁻³. This may be the pristine matter out of which comets and some asteroids formed while asteroids that formed closer to the sun had progressively lower fractions of volatiles. This gives us a definite model of interplanetary and cometary dust material considering that comets and asteroids are the likely "parents" or "grandparents" of most of today's meteoroids and zodiacal dust. When we consider that volatile ices have evaporated from dust located inside of the asteroid belt (Gustafson, 1994), we can expect the dust particles to be loosely packed aggregates or, at least, to have a highly porous structure. Cometary material, having formed far out in the nebula should be the most porous since they acquired a full complement of condensed volatiles and aggregated under conditions of low orbital velocities.

Based on growing evidence that most IDPs collected in the Earth's stratosphere are from the Koronis and Themis Hirayama families of asteroids (Dermott et al., this volume), it appears that S and C-type asteroids also produce aggregate type dust that is somewhat porous when it arrives at 1 AU. Our hypothesis is therefore that dust from comets and most undifferentiated asteroids are a mixture of silicates and a carbonaceous compound that may be similar to Greenberg's "yellow stuff" (Greenberg & Hage, 1990). The silicate material is optically represented by any material with refractive index m near $1.7 - 0.01i$ while the organic refractory as given by Greenberg & Hage has a refractive index closer to $1.8 - 0.2i$ in the visual.

According to this model, the structure of cometary dust is that of aggregates of silicate spheres coated with an absorbing refractory. While the packing factor of unaltered cometary material can be estimated to be 0.1 (i.e., 90% void, Greenberg & Hage, 1990), some cometary dust can be expected to be more densely packed. Gustafson (1990, 1994) suggested that the Geminid meteoroids are densely packed flakes produced on the surface of a choking comet. Freshly liberated dust particles from the receding ice surface get tangled in the interstices of particles that have not yet left the surface. The result is a layer of packed dust that is free of ice and that will soon choke the gas flow. The gas pressure builds up forcing the grains ever tighter until the mantle breaks into pieces that are hurled away explosively. Transient mantling where a dust mantle is blown off as soon as it forms was noticed in thermodynamic modeling of the mantling process by Rickman et al. (1990). Explosive ejection after pressure has built up sufficiently to break the mantle may also be an explanation for the high ejection velocities that are persistently found for meteoroids (e.g., Williams, this volume; Adolfsson & Gustafson, this volume).

A range of packing factors may be expected for asteroid dust. Given the average composition and high density of chondritic breccia (~ 3 g cm⁻³), they may be modeled as a compact mixture of the same refractories as the cometary dust (Figure 1). Average bulk densities of 2.1 ± 0.2 g cm⁻³ for S-type asteroids, given by Standish & Hellings (1989) as a preliminary value based on asteroid perturbation on the orbit of Mars, can allow for 15% by mass of water ice or a ~ 0.8 packing. The average bulk density obtained for C-type asteroids, 1.7 ± 0.5 g cm⁻³, leaves room for all the volatile ice in the primordial mixture or a packing factor as low as 0.7.



Figure 1. Microwave analog model of a comet mantle fragment or an S-type asteroid dust particle that is 8 micron across. Submicron silicate "interstellar" grain cores are embedded in an organic refractory material.

In conclusion, we have a working model for interplanetary dust material and can thus concentrate our light scattering investigations on materials with refractive indexes around some definite values. We conclude that the dust models should consist of two components arranged in the form of aggregates that range from compact to 90% porosity. Silicates are likely to be in the form of ~ 0.1 micron size spheres with the organic refractory as a coating. It is possible that the elongated structure of interstellar dust is preserved in the most pristine cometary material in the form of linear arrays of spheres. Our interplanetary dust models are therefore a mixture of materials arranged so that inhomogeneities are in the size range of resonance scattering in the visual, but close to the Rayleigh limit, in the infrared. The optical modeling of the material is therefore among the most challenging conceivable.

3. The Microwave Laboratory at the University of Florida

The experimental determination of scattered electromagnetic radiation from a known target illuminated by a known source is essential to test new scattering theories and to investigate the scattering by the great majority of particle morphologies for which a theory has not yet been devised. Precise control over all relevant parameters makes systematic investigations possible. The main obstacle to overcome is the mechanical precision required and the difficulty to handle particulates on the micron and sub-micron size scale. However, it has long been realized that dimensions in theoretical formulations of the electromagnetic scattering problem are only encountered as a ratio to the wavelength. This allows us to perform the experiment at the wavelength of our choice as long as we scale all target dimensions to the laboratory wavelength. Known as the principle of electromagnetic similitude, this was the basis for a series of highly successful single frequency microwave analog measurements in the X-band (3.18 cm wavelength)

initiated by J. M. Greenberg in the 1950s and in the Ka-band (8 mm) by R. H. Giese in the 1970s (see review by Zerull, 1985).

The new Microwave Scattering Facility at the Laboratory for Astrophysics of the University of Florida covers the entire w-band from 2.5 mm to 4 mm wavelength. This range corresponds to the visual spectrum shifted by a factor $\sim 10^4$ toward longer wavelengths. The fully automated measurements yield all elements of the scattering matrix from forward scattering (0 degrees) to 168 degrees. Corresponding to sizes from submicron to 30 micron across in the visual, targets can span over a much broader interval than in the earlier laboratories. The component arrangement we use is driven by mechanical and thermal stability considerations and is similar to that of a bi-static radar mounted on a rigid mechanically isolated and temperature compensated frame. We seek to approach the idealized conditions of electro-magnetic scattering that are commonly assumed in theoretical works, i.e., that of a monochromatic and flat incident wave to simulate a distant source of illumination. The parameters in the scattering matrix are easily separated when the electric vector is fully confined to the plane containing the Poynting vectors of the incident and detected scattered radiation and the measurement repeated with the field polarized perpendicular to this plane. The detector should be similarly sensitive to only one polarization direction at a time and sensitive to radiation propagating in a single direction. Measurement of the scattering cross section and phase retardation in the scattered wave as a function of scattering direction, at all four combinations of polarization, completely describes the scattering process.

The transmitting antenna is fixed with the receiving antenna sweeping an arc about the scatterer located at the intersection of the two beams. The fixed transmitting antenna is on the right in Figure 2a and the schematic drawing in Figure 2b. The mobile receiving antenna depicted to the left, intercepts scattered radiation from the target. Both ends have identical full band-width conical horn antennae and associated optics. A Fresnel lens produces a nearly flat wavefront over a 20 to 25 cm diameter spherical volume surrounding the target although the center of the target is only 135 cm from the antenna aperture. The effect of an identical Fresnel lens on the receiving antenna is to increase the sensitivity to radiation propagating in a single direction, i.e., the angular resolution is increased compared to a configuration using a direction insensitive detector. The resulting beams have ~ 15 db power reduction as close as 1 degree from the forward direction and sidelobes near 2 degrees are suppressed by 30 db. The narrow beams minimize stray radiation and reflections from surrounding structures are further reduced using anechoic material. The drawback of the broad-band narrow beam antennas is that they act in part as depolarizers so that up to 20% of the radiation passing through the horn may change its state of polarization. To remedy this, a polarizing filter is placed in front of the Fresnel lens to assure that both the transmitted and received radiation is linearly polarized. Each set of horn-lens-polarizer assembly can be rotated around the symmetry axis of the horn antenna so that the direction of polarization of transmitted and received radiation can be independently controlled. Because both the amplitude and phase of the scattered radiation is measured, the scattering process is completely characterized. All cross sections and efficiency factors (i.e., for absorption, scattering, extinction, radiation pressure, and the asymmetry factor) can be obtained from the forward scattering measurements in combination with

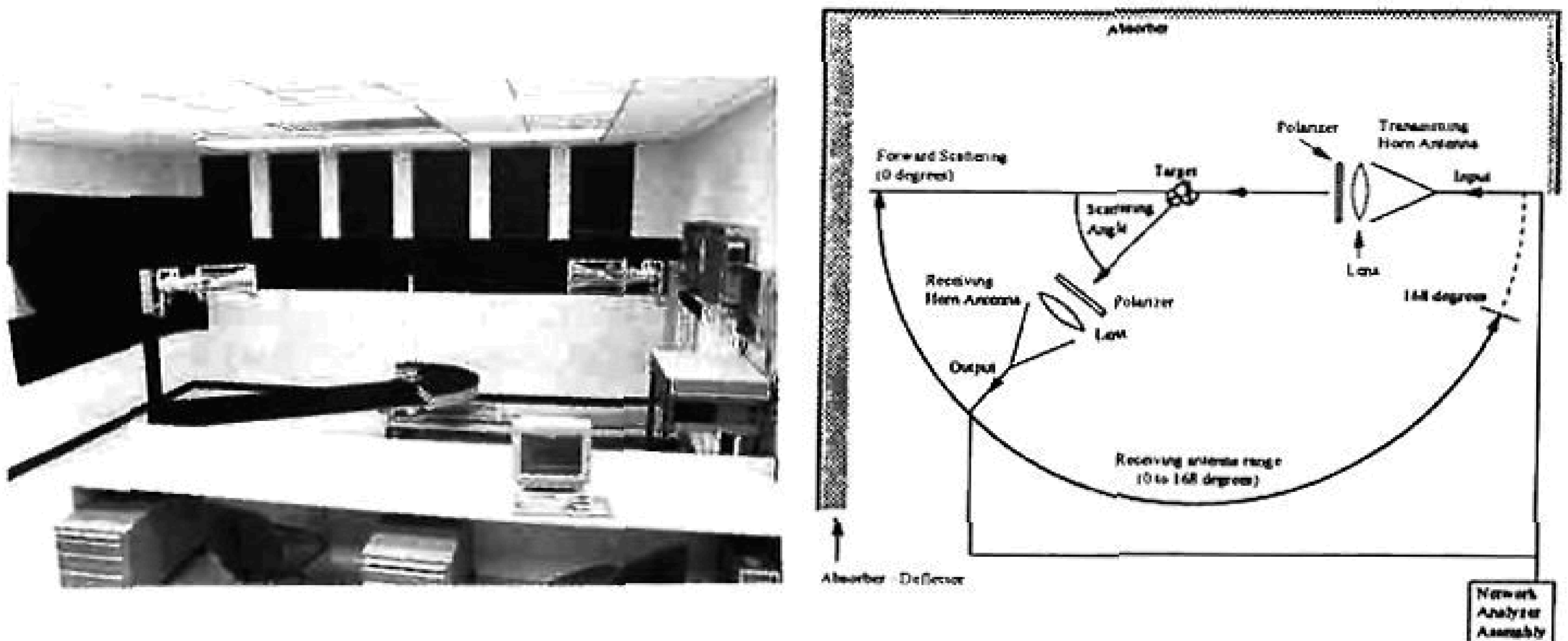


Figure 2. (a) Photograph showing the microwave analog scattering facility. (b) Schematic of the facility.

angular coverage. A more extensive description of the laboratory including the signal processing and a comparison to Mie-theory is given by Gustafson (1996).

4. A Compact Zodiacal Dust Particle Model

Laboratory data obtained using the microwave laboratory at Bochum, Germany, already gave a hint that compact dust models also can reproduce the general Rayleigh-like polarization shape of zodiacal dust. Figure 3 shows how the angular distribution of brightness and polarization shifts only slightly as an aggregate consisting of 500 individual spheres corresponding to silicates is coated by successively thicker layers of an absorbing compound representing the organic refractory mantle. A Rayleigh-Gans estimate of the contribution by the individual spheres show that they are practically invisible inside the thickest mantle and are thus not responsible for the polarization pattern.

While the model of Figure 3 corresponds to ~ 1.5 micron across at visual wavelengths, the optical properties of larger more realistic zodiacal dust models are at issue. We show data for the particle model in Figure 1, representing an 8 micron comet mantle fragment or S-type asteroid dust particle. Figure 4a shows polarization data corresponding to blue light obtained in the new microwave laboratory. While we see that the maximum has shifted to close to 65 degrees, the general shape is preserved. Figure 4b shows how the polarization remains essentially color independent throughout the visual range. A caution is due in that the refractive index of real materials may vary across the wavelength interval while the laboratory material is relatively insensitive, i.e., gray. On the other hand, many silicates are gray and organic refractories range from reddish yellow (Greenberg, private communication) to black (e.g., tar). Figure 5 shows that the brightness distribution appears to be neutral (gray) through most of the visual range except at the very shortest wavelengths where the brightness falls off, i.e., the particle would appear slightly red. This is at least qualitatively in agreement with observations of the zodiacal light. Detailed comparisons will

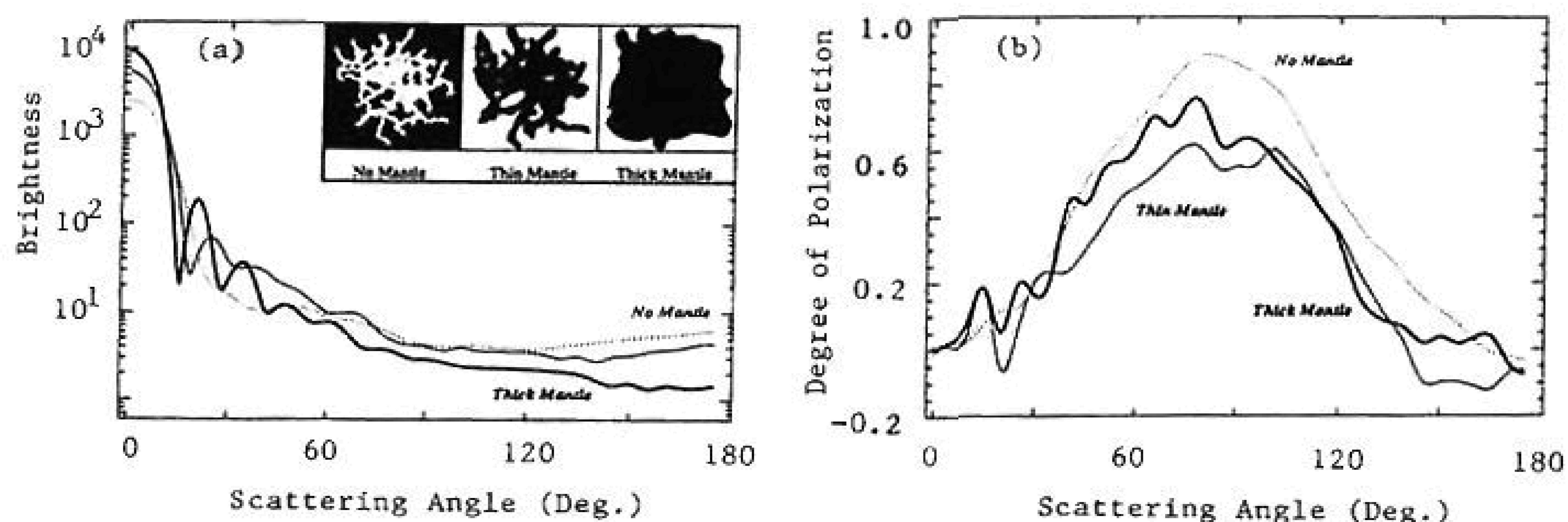


Figure 3. Effect of coating a 500 silicate sphere aggregate with an organic refractory mantle: (a) Brightness. (b) Polarization.

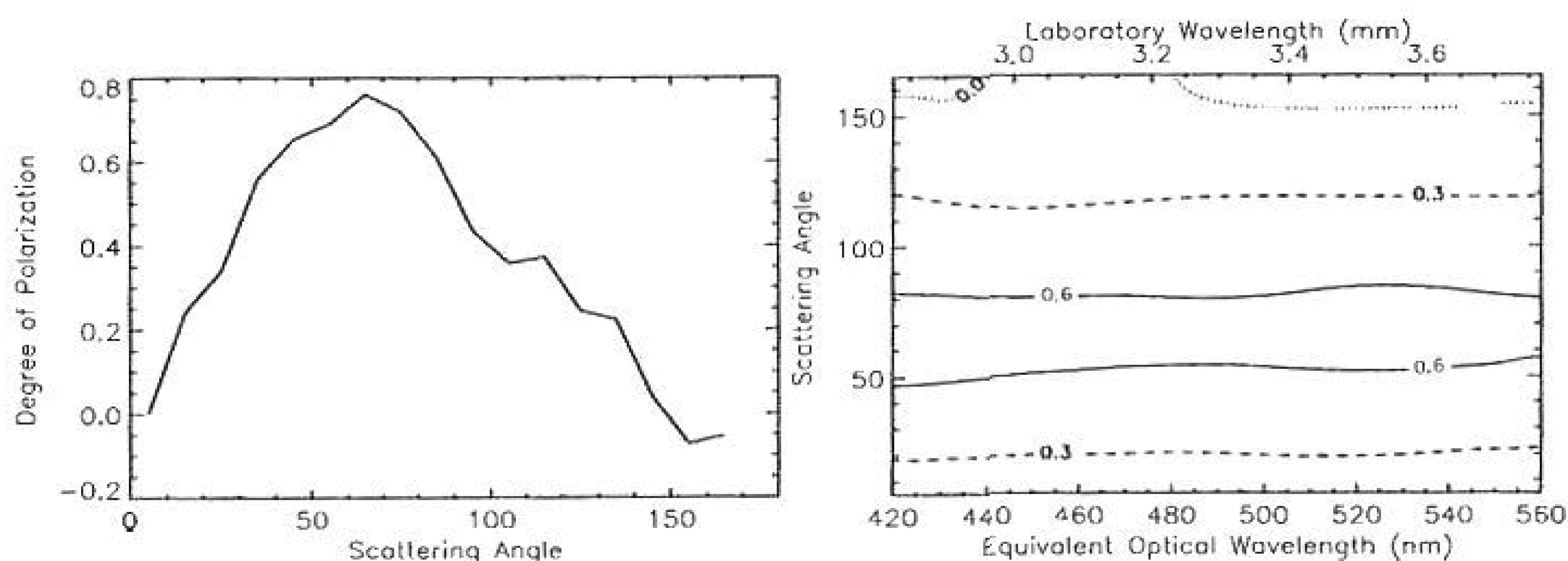


Figure 4. Degree of polarization of the S-type asteroid dust particle model shown in Figure 1: (a) In Blue light. (b) Across the visual range.

await until we have a range of laboratory data that can simulate a distribution of particles. Current measurements in the laboratory will produce both brightness and polarization data for our models of C- and D- type asteroid dust particles as well as for compact (mantle fragment) and fluffy ("Bird's-Nest" -type) cometary dust.

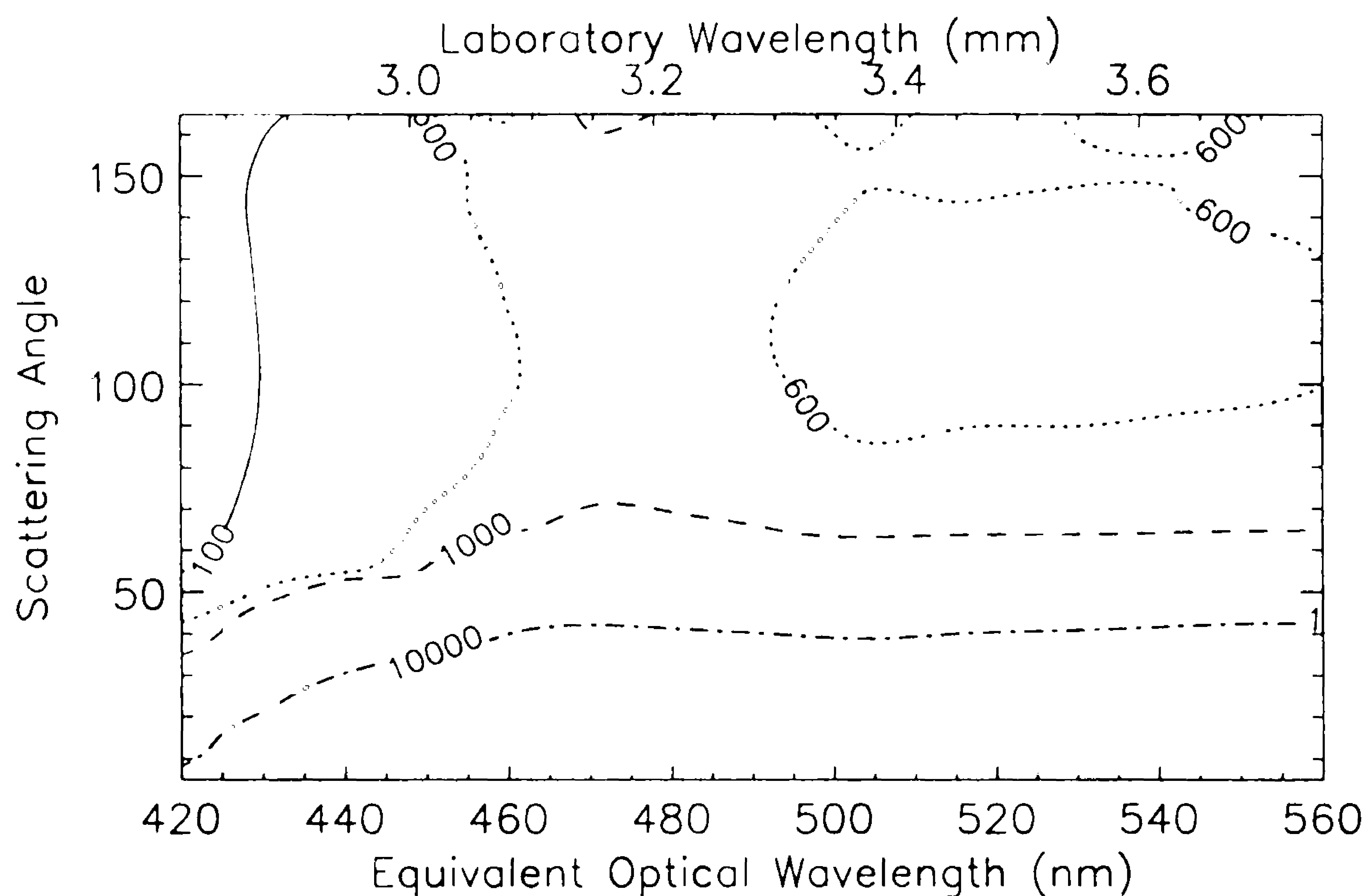


Figure 5. Scattered brightness across the visual range for the S-type asteroid dust particle model shown in Figure 1.

await until we have a range of laboratory data that can simulate a distribution of particles. Current measurements in the laboratory will produce both brightness and polarization data for our models of C- and D- type asteroid dust particles as well as for compact (mantle fragment) and fluffy ("Bird's-Nest" -type) cometary dust.

Acknowledgments. This research is supported by NASA's Planetary Atmospheres Program through grant NAGW-2482.

References

- Greenberg, J. M. 1988, in "Dust in the Universe", M. Bailey & D.A. Williams, Cambridge: Cambridge Univ. Press, 121
- Greenberg, J. M. & B. Å. S. Gustafson 1981, *A&A*, 93, 35
- Greenberg, J. M. & J. I. Hage 1990, *ApJ*, 361, 260
- Gustafson, B. Å. S. 1990, in "Asteroids, Comets, Meteors III", C.-I. Lagerkvist et al., Uppsala: Uppsala University Reprocentralen HSC, 523
- Gustafson, B. Å. S. 1994, *Annu. Rev. Earth Planet. Sci.*, 22, 553
- Gustafson, B. Å. S. 1994, *Jour. Quant. Spect. Rad. Transf.*, 55:5, 663
- Rickman, H., J. A. Fernández & B. Å. S. Gustafson 1990, *A&A*, 237, No. 2, 524
- Seab, C. G. 1987, in "Interstellar Processes", D.J. Hollenbach & H.A. Thronson, Dordrecht: Reidel, 491
- Standish, E. M.-Jr & R. W. Hellings 1989, *Icarus*, 80, 326
- Xu, Y.-L. 1995, *Appl. Optics*, 34, 4573
- Zerull, R. H. 1985, in "Properties and Interactions of Interplanetary Dust", R. H. Giese & P. Lamy, Dordrecht: Reidel, 197